Effects of SrRuO3 layer on retention properties of (Bi, Pr)(Fe, Mn)O3 film capacitor at high temperature

ECS Solid State Letters, **4** (5) N1-N4 (2015)
2162-8742/2015/4(5)/N1/4/$33.00 © The Electrochemical Society

Effects of $SrRuO_3$ Layer on Retention Properties of $(Bi,Pr)(Fe,Mn)O_3$ Film Capacitor at High Temperature

Keisuke Nomura, Yuki Kondo, Takeshi Kawae,[z] and Akiharu Morimoto

Graduate School of Natural Science and Technology, Kanazawa University, Kakuma-machi, Kanazawa, Ishikawa 920-1192, Japan

We investigated the effects of a $SrRuO_3$ (SRO) layer on the retention properties of $(Bi,Pr)(Fe,Mn)O_3$ (BPFM) film capacitors under high temperature conditions. The dielectric constant of the BPFM film capacitor was increased by the introduction of the SRO layer. In addition, the Pt/BPFM/SRO/Pt capacitor showed polarization losses of only 6.4% in both polarization directions after a retention time of 10^4 s at 400°C, resulting in symmetrical switching behavior. These results imply that the introduction of the SRO layer is effective in suppression of the formation of an interfacial layer between BPFM and Pt.

Manuscript submitted January 30, 2015; revised manuscript received February 25, 2015. Published March 5, 2015.

Ferroelectric random access memory (FeRAM) is currently attracting significant interest as a non-volatile memory technology that offers both low power consumption and high-speed operation. Recently, there have been attempts to apply FeRAM in the medical field because the ferroelectric domain of the devices has superior radiation hardness. The stability of the ferroelectric polarization is considered to be one of the most important factors that would enable wider expansion of the application range of FeRAM devices. The data integrity of non-volatile memories is typically required to be guaranteed for more than ten years over a wide range of temperatures, ranging from −10 to 70°C for consumer applications and from −40 to 85°C for industrial applications. In addition, memory devices that can store data at higher temperatures are also required to act as ID tags for use in the heat-treatment lines of factories that are used to manufacture various products. Thus, the ability to maintain a poled polarization state over time at higher temperatures is required for further expansion of the application areas of FeRAM devices.

In general, after polarization reversal by the application of an electric field, the number of polarization charges in a ferroelectric capacitor decreases with increasing retention time.[1–4] In addition, the remnant polarization decay process is accelerated when the capacitor is kept at higher temperatures.[1,2] According to previous reports, the remnant polarization decay is caused by the generation of polarization back-switching by the internal field that is formed by the redistribution of defect charges near the metal-ferroelectric interface during the retention period.[1,3] When the number of polarization charges in the FeRAM devices decreases below a specific threshold level, the memory of the bit is lost. Therefore, polarization loss is an important factor in the expansion of FeRAM device application areas over a wide range of temperature.

In previous work, we have noted that $BiFeO_3$ (BFO) with its large spontaneous polarization (∼100 μC/cm^2), high Curie temperature (830°C), and large coercive field (300 kV/cm) is a ferroelectric material that can achieve superior retention properties even at high temperatures.[6–9] The large spontaneous polarization of BFO enables further integration of FeRAM devices. In addition, the remnant polarization is expected to be stable at high temperatures because of the large coercive field of BFO, which is closely correlated to the barrier height of the polarization loss on a thermal dynamics basis.[10]

In our previous study, we reported on the high temperature retention properties of a Pt/$(Bi,Pr)(Fe,Mn)O_3$ (BPFM)/Pt capacitor that used (Pr,Mn)-doped BFO prepared by the chemical solution deposition (CSD) method as a ferroelectric layer.[11] Here, the BPFM material has been modified to improve the insulation performance of BFO.[12,13] As a result, the Pt/BPFM/Pt capacitor showed good retention performance with low polarization losses even at temperatures above 400°C. However, differences in the polarization losses, which depend on the polarization directions during the retention time, were observed in the retention performance of the Pt/BPFM/Pt capacitor. Asymmetric retention properties have often been reported in ferroelectric capacitors with asymmetrical boundary conditions.[4] According to a previous study, atomic diffusion from the ferroelectric layer to the Pt bottom electrode occurred when ferroelectric thin films were deposited on the Pt/Si substrate by the CSD method.[14] Because the electrode-ferroelectric interface in a ferroelectric capacitor strongly affects the device's retention performance,[1,3–5] we presumed that the asymmetric switching behavior of the Pt/BPFM/Pt capacitor was mainly caused by differences between the electrode-ferroelectric interface structures at the top and bottom electrodes due to atomic diffusion. To solve the problem of atomic diffusion through the interface, oxide electrode materials such as RuO_2 and $SrRuO_3$ (SRO) were often used to suppress interface defects.[15] Therefore, we have attempted to introduce an SRO layer with high a work function and high electrical conductivity on the Pt bottom electrode to act as a barrier layer and obtain a good ferroelectric/bottom-electrode interface in the BPFM film capacitor, which resulted in SRO/Pt layered bottom electrodes. In this study, we report the effects of the SRO layer on the retention properties of a BPFM film capacitor at high temperatures.

Experimental

A 60-nm-thick SRO layer was deposited on a Pt-coated Si(100) substrate at room temperature (RT) by the pulsed laser deposition (PLD) method. Then, the BPFM thin film was prepared on the SRO/Pt/Si(100) substrate by the CSD method. A BPFM solution with composition of $(Bi_{0.9}Pr_{0.1})(Fe_{0.97}Mn_{0.03})O_3$ was spin-coated at 3000 rpm for 30 s; this process was followed by a drying procedure at 240°C for 5 min and a pyrolysis process at 365°C for 10 min in the ambient atmosphere. These processes were repeated ten times, resulting in a film thickness of 220 nm. Pt top electrodes with areas of 2.5×10^{-5} cm^2 were deposited on the BPFM thin film at room temperature (RT) by the PLD method using a shadow mask, to obtain the metal-ferroelectric-metal capacitor structure.

The polarization vs. electric field (*P-E*) curves of the specimen were measured using a ferroelectric test system (Toyo FCE-3) with a measurement frequency of 5 kHz. Capacitance vs voltage (*C-V*) curves were measured using a precision LCR meter (Agilent 4284A) at 1 MHz. The crystal structure was determined by X-ray diffraction (XRD; Rigaku Smart Lab) analysis with Cu Kα radiation.

Results and Discussion

Figure 1 shows the XRD 2θ-ω scanning patterns of the Pt/BPFM/SRO/Pt capacitor. For comparison, the corresponding XRD 2θ-ω scanning patterns of a Pt/BPFM/Pt capacitor are also shown in the figure. The BPFM thin film was found to be polycrystalline and formed without any impurity phases such as Bi_2O_3 and $Bi_2Fe_4O_9$ in both specimens.[16] In addition, no significant differences in crystallization between the two specimens were observed with respect to the

[z]E-mail: kawae@ec.t.kanazawa-u.ac.jp

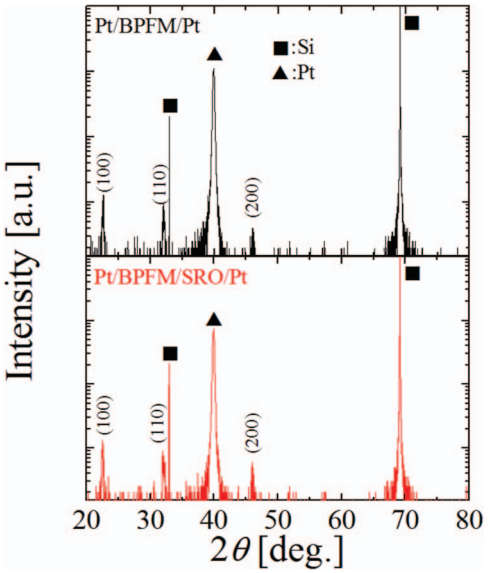

Figure 1. XRD patterns for the Pt/BPFM/SRO/Pt and Pt/BPFM/Pt capacitors. Symbols indicate the Si substrate and the Pt thin films.

BPFM thin film. Therefore, we consider that the introduction of the SRO layer hardly had any effect on the crystallization of the BPFM thin film.

Figure 2 shows the *P-E* curve for the Pt/BPFM/SRO/Pt capacitor, as measured at RT. To investigate the effects of introduction of the SRO layer, the curve of the Pt/BPFM/Pt capacitor is also shown in the figure. Well-saturated hysteresis loops are observed in both capacitors. The remnant polarization ($2P_r$) and the coercive field ($2E_c$) of the Pt/BPFM/Pt capacitor were 108 μC/cm^2 and 617 kV/cm, respectively, at the maximum electric field of 900 kV/cm. On the other hand, $2P_r$ and $2E_c$ in the Pt/BPFM/SRO/Pt capacitor were 132 μC/cm^2 and 490 kV/cm, respectively. As a result, we find that $2P_r$ was increased and $2E_c$ was reduced by the introduction of the SRO layer. Therefore, we confirmed that the SRO layer protects the ferroelectric/electrode interface and leads to improvement of the ferroelectric properties of the BPFM film capacitor.[17,18]

The retention properties of the specimens were performed using the ferroelectric test system with conventional rectangular pulses.[1,11,19] The pulse train used for the retention measurements is shown in Fig. 3. After the application of a write pulse with pulse width t_0 to the capacitor at RT, the BPFM capacitor was maintained at the retention temperature of RT or at 400°C in a N_2 gas flow. Then, the retention time t_1 was varied from 10^{-3} to 10^4 s. For the read pulse, switching and non-switching pulses with pulse widths of t_0 were applied at RT,

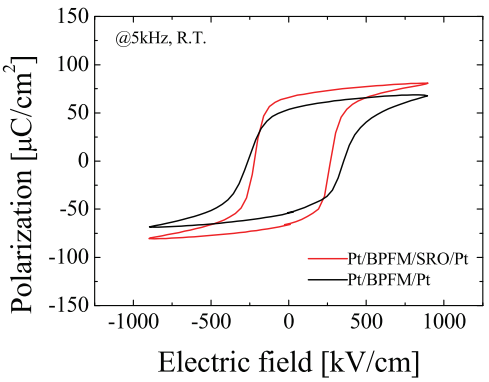

Figure 2. *P-E* curves of the Pt/BPFM/SRO/Pt and Pt/BPFM/Pt capacitors with measurement frequency of 5 kHz at RT.

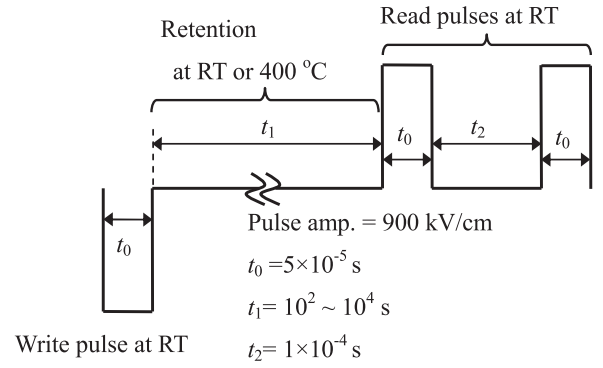

Figure 3. Pulse train used for retention measurement with the downward polarization ($-P_r$) state. The write and read pulses were applied at RT. The retention temperature was RT or 400°C. When the retention properties are measured while the polarization points in the upward direction (i.e., the $+P_r$ state), the polarities of the three pulses are reversed.

and the switching charges Q_{sw} were calculated from the difference between the observed switching polarization and the non-switching polarization. The pulse width t_0 and the pulse interval t_2 were 5 × 10^{-5} s and 1 × 10^{-4} s, respectively, and a pulse amplitude of 900 kV/cm was used to obtain sufficient polarization charges because the E_c of the specimen was approximately 250–300 kV/cm. Q_{sw} in the Pt/BPFM/SRO/Pt capacitor which was 127 μC/cm^2 at the maximum applied field of 900 kV/cm with a retention time t_1 of 10^{-3} s was found to be close to the $2P_r$ value of the specimen that was observed in the *P-E* curve.

Figure 4 shows the retention properties of the normalized Q_{sw} in the Pt/BPFM/SRO/Pt capacitor as a function of the retention time at RT. Here, the Q_{sw} value was normalized relative to that of Q_{sw} measured with t_1 of 10^{-4} s. The $+P_r$ state and the $-P_r$ state denote polarization vectors that point toward the top and the bottom electrodes, respectively, during the retention period. From the retention measurements at RT, we confirmed that the Pt/BPFM/SRO/Pt capacitor showed good retention properties as did the Pt/BPFM/Pt capacitor.[11] In addition, the rapid polarization losses and short retention times that can be caused by a depolarization field were not observed.[1,4]

Secondly, we measured the retention performances of the Pt/BPFM/SRO/Pt capacitor at a retention temperature of 400°C. Figure 5 shows the retention properties of the normalized Q_{sw} in the Pt/BPFM/SRO/Pt capacitor as a function of t_1 at 400°C. For comparison, the retention properties of the Pt/BPFM/Pt capacitor under the same conditions are also shown in the figure. The Pt/BPFM/Pt capacitor retained more than 90% of Q_{sw} with a t_1 of 10^4 s at 400°C in both the $+P_r$ and $-P_r$ states. However, the polarization losses of the $+P_r$

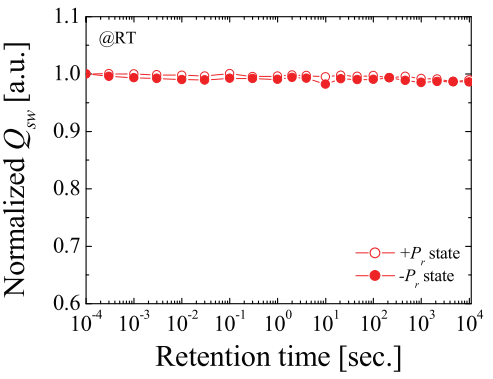

Figure 4. Retention properties of normalized Q_{sw} in the Pt/BPFM/SRO/Pt capacitor as a function of retention time. The retention temperature was RT. Upward and downward polarizations are denoted by the $+P_r$ state and the $-P_r$ state, respectively.

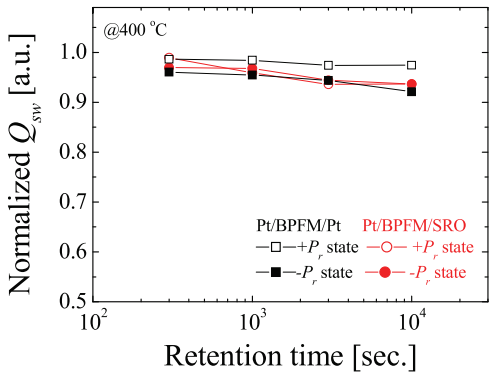

Figure 5. Normalized Q_{sw} retention properties in the Pt/BPFM/SRO/Pt and Pt/BPFM/Pt capacitors as a function of retention time. The retention temperature was 400°C. Upward and downward polarizations are denoted by the $+P_r$ state and the $-P_r$ state, respectively.

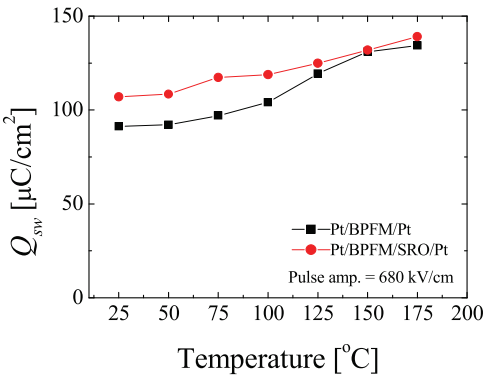

Figure 6. Temperature dependence of Q_{sw} in the Pt/BPFM/SRO/Pt and Pt/BPFM/Pt capacitors. The pulse amplitude was 680 kV/cm.

and $-P_r$ states were approximately 3% and 8% respectively, which resulted in asymmetric switching behavior. One of the causes of this asymmetric switching behavior is the difference in the built-in bias of the ferroelectric-top and bottom electrode contacts in the Pt/BPFM/Pt capacitor. While the Pt/BPFM/Pt capacitor is a symmetrical structure from a material view point, the observed results demonstrate that the effective work functions of the two electrodes are different. We attribute this difference between the effective work functions of the two electrodes to the thermal conditions during specimen fabrication. Another cause of highly asymmetric switching behavior in the Pt/BPFM/Pt capacitor is the existence of an interfacial layer between the BPFM film and the Pt bottom electrode. As mentioned above, it is known that atomic diffusion often occurs into the bottom electrode through the grain boundary of the Pt bottom electrode during the ferroelectric thin film fabrication process. This atomic diffusion forms an interfacial layer with a low dielectric constant between the ferroelectric thin film and the bottom electrode, which reduces the screen charges in the bottom electrode. Because reduction of the screen charges in the bottom electrode causes enhancement of the depolarization field in a ferroelectric capacitor,[1,4,20] the asymmetric switching behavior of the Pt/BPFM/Pt capacitor was enhanced. In contrast, the polarization losses were approximately 6.4% with t_1 of 10^4 s at 400°C in both the $+P_r$ and $-P_r$ states for the Pt/BPFM/SRO/Pt capacitor. This highly symmetrical switching behavior in the Pt/BPFM/SRO/Pt capacitor demonstrates that the SRO layer is effective in suppressing the atomic diffusion. In addition, the similar work functions of Pt (5.4 eV) and SRO (5.1 eV) could also contribute to the symmetrical switching behavior of the Pt/BPFM/SRO/Pt capacitor.[21,22]

To further confirm that the introduction of the SRO layer suppressed the atomic diffusion, we calculated the dielectric constants of the two capacitors. When an interfacial layer with a low dielectric constant is formed because of atomic diffusion between the BPFM thin film and Pt bottom electrode, the dielectric constant of the Pt/BPFM/Pt capacitor should be smaller than that of the Pt/BPFM/SRO/Pt capacitor. The results of *C*-*V* measurements showed that the dielectric constants of the Pt/BPFM/Pt and Pt/BPFM/SRO/Pt capacitors were 115 and 139, respectively. This result implies that the formation of the interfacial layer with the low dielectric constant was prevented by the introduction of the SRO layer. Hence, we consider that the good BPFM/SRO interface suppresses the depolarization field, which results in the symmetrical switching behavior that was observed for the Pt/BPFM/SRO/Pt capacitor.

Although symmetrical switching behavior was obtained by introduction of the SRO layer, the polarization losses with t_1 of 10^4 s at 400°C were slightly larger than those observed for the $+P_r$ state for the Pt/BPFM/Pt capacitor. We therefore measured the measurement temperature dependence of Q_{sw} for all specimens, to investigate the cause of the larger polarization losses in the Pt/BPFM/SRO/Pt capacitor. In these measurements, conventional rectangular pulses were used along with the retention measurements. Here, all pulses had a width of 5×10^{-5} s and t_1 was 10^{-3} s. After the specimens were poled toward the top electrode by application of the write pulse, two read pulses of opposite polarity were applied to obtain Q_{sw}. This pulse train with amplitudes of 680 kV/cm was applied in the temperature range from RT to 175°C. Figure 6 shows Q_{sw} as a function of the measurement temperature for the Pt/BPFM/SRO/Pt and Pt/BPFM/Pt capacitors. As shown in the figure, a rapid increase in Q_{sw} was observed above 100°C for the Pt/BPFM/Pt capacitor. This trend indicates that reversal of the domains that were pinned by defects occurred because of the elevated thermal energy.[23–25] In contrast, no rapid increase in Q_{sw} was observed for the Pt/BPFM/SRO/Pt capacitor with increasing measurement temperature. When considering the dielectric constants of the two capacitors, the effective applied voltage across the BPFM film in the Pt/BPFM/SRO/Pt capacitor is higher than that in the Pt/BPFM/Pt capacitor. We should note that a similar trend was observed for even the smaller pulse amplitudes (450 kV/cm). Based on these results, it is suggested that the Pt/BPFM/SRO/Pt capacitor requires lower activation energy for polarization reversal than the Pt/BPFM/Pt capacitor. This agrees well with the magnitude correlation of $2E_c$ between the two specimens, shown in Fig. 1. The lower polarization reversal activation energy of the Pt/BPFM/SRO/Pt capacitor means that polarization reversal induced by the depolarization field occurs readily. Hence, the larger polarization losses for the Pt/BPFM/SRO/Pt capacitor were due to the low polarization reversal activation energy caused by the introduction of the SRO layer, which reduces the density of pinning site with deep energy level in the capacitor structure. In future work, to solve the problem of these large polarization losses, it will be necessary to improve the retention properties of the Pt/BPFM/SRO/Pt capacitor through the introduction of artificial trap sites by elements substitution.[26]

Conclusions

We introduced the SRO layer on the Pt bottom electrode to improve the asymmetric switching behavior of the Pt/BPFM/Pt film capacitor. The polarization losses that were measured with a retention time of 10^4 s at 400°C for the Pt/BPFM/SRO/Pt capacitor were approximately 6.4% in both the $+P_r$ and $-P_r$ states. Moreover, symmetrical switching behavior was obtained as a result of the introduction of the SRO layer. The observed symmetrical switching was mainly caused by the improvement in the ferroelectric/bottom electrode interface due to introduction of the SRO layer.

References

1. J. M. Benedetto, R. A. Moore, and F. B. McLean, *J. Appl. Phys.*, **75**, 460 (1994).
2. Y. Shimada, M. Azuma, K. Nakao, S. Chaya, N. Moriwaki, and T. Otsuki, *Jpn. J. Appl. Phys.*, **36**, 5912 (1997).

3. B. S. Kang, D. J. Kim, J. Y. Jo, T. W. Noh, Jong-Gul Yoon, T. K. Song, Y. K. Lee, J. K. Lee, S. Shin, and Y. S. Park, *Appl. Phys. Lett.*, **84**, 3127 (2004).
4. A. Gruverman and M. Tanaka, *J. Appl. Phys.*, **89**, 1836 (2001).
5. A. Q. Jiang and T. A. Tang, *J. Appl. Phys.*, **104**, 024104 (2008).
6. J. Wang, J. B. Neaton, H. Zheng, V. Nagarajan, S. B. Ogale, B. Liu, D. Viehland, V. Vaithyanathan, D. G. Schlom, U. V. Waghmare, N. A. Spaldin, K. M. Rabe, M. Wuttig, and R. Ramesh, *Science*, **299**, 1719 (2003).
7. K. Y. Yun, D. Ricinschi, T. Kanashima, and M. Okuyama, *Appl. Phys. Lett.*, **89**, 192902 (2006).
8. K. Y. Yun, D. Ricinschi, T. Kanashima, M. Noda, and M. Okuyama, *Jpn. J. Appl. Phys.*, **43** L647 (2004).
9. V. V. Shvartsman, W. Kleemann, R. Haumont, and J. Kreisel, *Appl. Phys. Lett.*, **90**, 172115 (2007).
10. M. Vopsaroiu, J. Blackburn, M. G. Cain, and P. M. Weaver, *Phys. Rev. B*, **82**, 024109 (2010).
11. Y. Nomura, K. Nomura, K. Kinoshita, T. Kawae, and A. Morimoto, *Phys. Status Solidi RRL*, **8**, 536 (2014).
12. T. Kawae, Y. Terauchi, T. Nakajima, S. Okamura, and A. Morimoto, *J. Ceram. Soc. Jpn.*, **118**, 652 (2010).
13. T. Kawae, H. Kawasaki, T. Nakajima, N. Tokuda, S. Okamura, A. Morimoto, and Y. Takano, *Jpn. J. Appl. Phys.*, **51**, 09LA08 (2012).
14. S. G. Lee, K. T. Kim, and Y. H. Lee, *Thin Solid Films*, **372**, 45 (2000).
15. S. N. Ryoo, S. G. Yoon, and S. H. Kim, *Appl. Phys. Lett.*, **83**, 2880 (2003).
16. A. Ablat, E. Muhemmed, C. Si, J. Wang, H. Qian, R. Wu, N. Zhang, R. Wu, and K. Ibrahim, *J. Nanomater.*, **2012**, 123438 (2012).
17. S. Kim, J. Koo, S. Shin, and Y. Park, *Appl. Phys. Lett.*, **87**, 212910 (2005).
18. J. Karthik, A. R. Damodaran, and L. W. Martin, *Adv. Mater.*, **24**, 1610 (2012).
19. I. Stolichnov, A. K. Tagantsev, E. Colla, N. Setter, and J. S. Cross, *J. Appl. Phys.*, **98**, 084106 (2005).
20. A. M. Bratkovsky and A. P. Levanyuk, *Appl. Phys. Lett.*, **89**, 253108 (2006).
21. D. Gu and S. K. Dey, *Appl. Phys. Lett.*, **89**, 082907 (2006).
22. M. Tapajna, P. Pisecny, R. Luptak, K. Husekova, K. Frohlich, L. Harmatha, J. C. Hooker, F. Roozeboom, and J. Jergel, *Mat. Sci. Semicon. Proc*, **7**, 271 (2004).
23. B. J. Rodriguez, Y. H. Chu, R. Ramesh, and S. V. Kalinin, *Appl. Phys. Lett.*, **93**, 142901 (2008).
24. A. Gruverman, B. J. Rodriguez, R. J. Nemanich, and A. I. Kingon, *J. Appl. Phys.*, **92**, 2734 (2002).
25. J. W. Park, S. H. Baek, P. Wu, B. Winchester, C. T. Nelson, X. Q. Pan, L. Q. Chen, T. Tybell, and C. B. Eom, *Appl. Phys. Lett.*, **97**, 212904 (2010).
26. T. Kawae, Y. Terauchi, H. Tsuda, M. Kumeda, and A. Morimoto, *Appl. Phys. Lett.*, **94**, 112904 (2009).